Available online at www.sciencedirect.com

jmr&t Journal of Materials Research and Technology

journal homepage: www.elsevier.com/locate/jmrt

Review Article

Mineral characterization of low-grade gold ore to support geometallurgy

Fabrizzio R. Costa[*], *Guilherme P. Nery*, *Cleyton de Carvalho Carneiro*, *Henrique Kahn*, *Carina Ulsen*

Universidade de São Paulo, Mining and Petroleum Engineering Department, Av. Prof. Mello Moraes, 2373, Butantã, 05508-030, Sao Paulo, SP, Brazil

ARTICLE INFO

Article history:
Received 2 May 2022
Accepted 18 October 2022
Available online 22 October 2022

Keywords:
Geometallurgy
SEM-based automated image analysis
Low-grade gold ore
Accessibility

ABSTRACT

SEM-based automated image analysis is one of the most comprehensive tools in mineralogical characterization and plays an important role in the mining sector, mainly due to its statistical robustness, reliability of results and rapid analysis compared to analogue methods. Mineralogical ore characterization, such as gold distribution, grain size and mode of occurrence, together with density separation, cyanidation and diagnostic leaching tests, are the key for the appropriate process design of the geometallurgy concept. The present research focuses on the development of a mineralogical characterization of low-grade gold ore (<0.5 g/t) using SEM-based automated image analysis (SEM-IA) to evaluate minerals association, gold exposure and elemental deportment by gold-bearing mineral as a support for the geometallurgy program. A set of 168 samples of low-grade carbonaceous seriticitic phyllite gold ore from an open pit mine located in Minas Gerais State, Brazil, was characterized. The geological units could be defined by the content of arsenic (<1000; 1000–2000; 2000–3000; 3000–4000 and >4000 ppm) due to a unique set of compositional properties, such as grain size, sulphide mineralogy and accessibility, which directly affect the metallurgical performance. The results demonstrated that there is a direct correlation between the arsenic grades and the gold content, as well as an influence of arsenic grades on gold accessibility. Furthermore, high arsenic content in gold grains tends to provide greater accessibility. Although gold grains occur mainly as inclusions in pyrite and arsenopyrite, they are rarely associated with other sulphide (pyrrhotite and galena).

1. Introduction

Geometallurgy is a multi-disciplinary approach that integrates geology and metallurgy information to incorporate principles of process mineralogy and ore characterization. As it serves as a tool for predictive geological block model and mineral processing performance, such approach is widely used in production management [1–4]. The geometallurgy concept has received increasingly more attention due to the

* Corresponding author.
E-mail addresses: fab.costa@usp.br, frcusp@yahoo.com.br (F.R. Costa).
https://doi.org/10.1016/j.jmrt.2022.10.085

development of modern mineralogical characterization techniques and equipment that contribute to the production of high-grade ores, predicting mineral processing characteristics, as well as to new ore discoveries, characterized as low-grade/high-tonnage deposits, which consequently reducing risks during the operation [5–7].

The most comprehensive method for mineralogical associations analysis for geometallurgical programs is the combination of scanning electron microscopy imaging with energy dispersive spectroscopy (SEM/EDS) and automated image analysis (SEM-IA) to determine mineral textures, mineral association, mineralogical composition, grain size distribution, exposure, liberation and elemental deportment by mineral [8–10].

Although the application SEM-IA has played an important role in the mining industry, mainly because of its rapid analysis, statistical robustness and reliability of results, it should be considered that the analysis is limited to two dimensions, even though the data are used to describe three-dimensional characteristics of samples, such as particle size, shape and composition. Therefore, a stereological bias in the two-dimensional analysis can result in overestimated data depending on the position in which the particle is exposed [11–13].

For gold ores, the classical concept of degree of liberation described by Gaudin [14] loses its meaning when the processes used for their recovery and extraction are based on specific properties of this element, such as leaching by alkaline solutions of cyanide. The classical definition of "mineral liberation" shows that in a population of particles of different mineral species, the degree of liberation of one of the species consists of the percentage of this mineral which occurs as free particles in relation to the total amount of this mineral in mixed or free particles. In Fig. 1 is illustrated different classes of particles phase and its perimeter exposed.

The term "exposed perimeter" is defined as the perimeter of a gold grain (in pixels) that is in contact with no other grain and must contain at least one pixel to be accounted for. The accessible gold is directly related to the gold possibly extracted by a leaching solution.

Petruk [15] reported that the main textures for gold deposits are: a) accessible – gold exposed by fractures and microfractures in rock matrix, b) locked but not encapsulated – gold in interstitial spaces between mineral grains or occurring on the boundary of different minerals, and c) encapsulated; gold grain locked in a host mineral. The implication of structurally bound gold extraction is that gold in interstitial spaces between sulphide or silicates grains will be improved with finer grinding to recover gold-bearing ores. The physical lock-up of gold can be overcome by ultra-fine grinding of the ore to liberate the locked gold or enable the complete destruction of the mineral when present in the solid solution within the mineral matrix in the form of molecular or "invisible" gold [16,17]. However, the ultra-fine grinding is a physical method for the exposed of locked gold, but due to high energy requirements it is an expensive operation.

For gold ores processed by hydrometallurgy, the term "accessibility" is more appropriate because the gold grain does not necessarily need to be free, but partially exposed to allow the access of a leaching solution through fracture or some other means that provide such access.

Fig. 2 illustrates different occurrences of the gold grain regarding the exposure of its perimeter for percolation of a cyanide solution. In Fig. 2 a is possible to observe that even though the gold grain is not free, it has a fracture for the solution percolation, making it accessible. Fig. 2b and c present

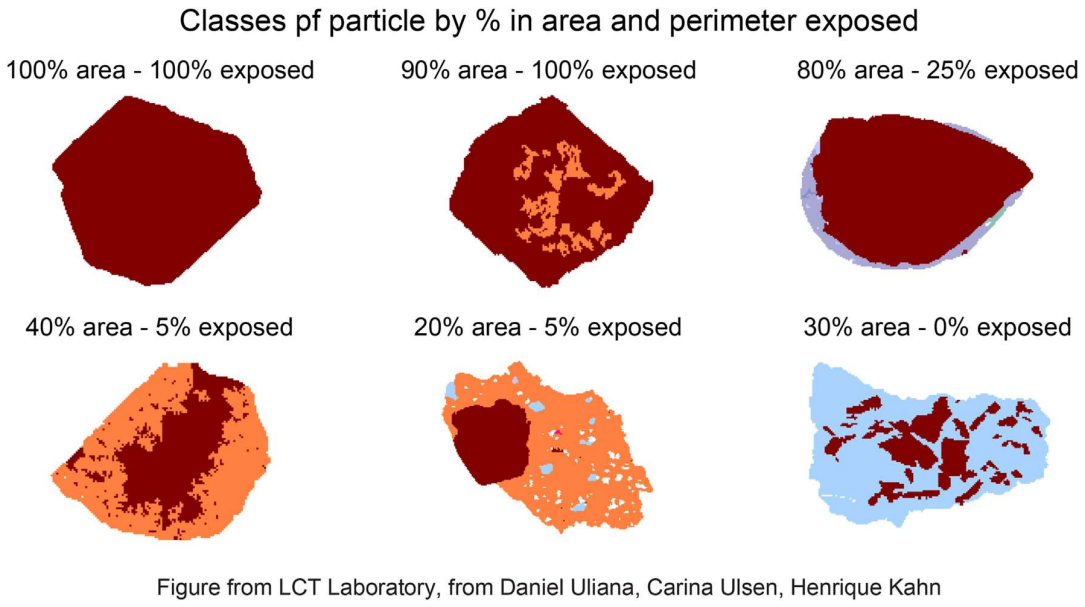

Fig. 1 – Schematic representation of classes of particles by percentage in area and perimeter exposed (phase of interest in brown)

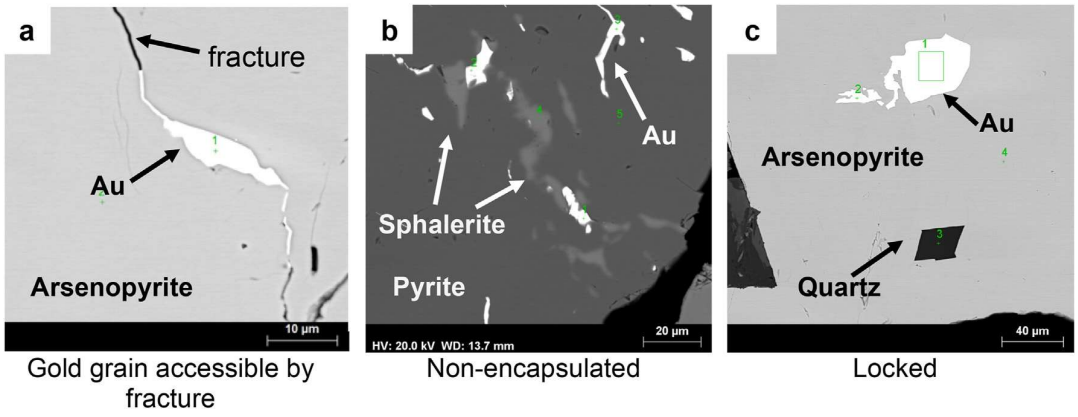

Fig. 2 – Accessibility of gold grain. (a) Gold grain with minimum exposure and accessibility, liable to be leached, (b) mixed particles with gold grains in contact with two or more phases, and (c) gold grain locked in arsenopyrite particle.

different ways of including gold grains into two-dimensional (2D) images. Fig. 2b indicates a gold grain that is not encapsulated, it is in contact of two or more phases, and Fig. 2c indicates a locked gold grain, which is locked into a single mineral. In these examples, the action of the solution would not be possible, as there is no facilitating/conducting for the percolation. Since it is a two-dimensional observation, the gold may be extractable by paths located in another part of the grain not visualized in the 2D image. Thus, information on gold accessibility by image analysis may be undersized or underestimated due to pixel size resolution.

Mineralogical characterization data obtained by SEM-IA validate a wide range of metallurgical techniques used to test the extractability of gold from gold ore, such as direct cyanidation, gravity separation and diagnostic leaching [16,18]. The direct cyanidation test is performed at different conditions (excess or controlled) and is able to indicate the amenability of the ore to gold extraction by cyanidation. Its results are comparable to those of gold grain exposure determined during SEM-IA [16].

The interpretation of leaching tests is sometimes difficult, especially if mineralogical characterization is not taken into consideration. As an example, we can cite the cyanidation tests used to quantify the gold associated with carbonaceous material and significant contents of aurostibite, arsenic sulphide minerals and oxygen-consuming pyrrhotite in minor occurrence. These sulphide interfere with the cyanidation process, consuming cyanide and oxygen, and thus forming passivation rims around gold grains during cyanidation. The increase of the cyanide consumption is related to the higher surface area of cyanide-consuming minerals or the presence of pyrrhotite that reacts with cyanide causing an undesirable increase in consumption.

This paper focuses on the study of gold grain characteristics and accessibility by SEM-IA and leaching tests to optimize mineral resource and as input to the geometallurgical program of a set of 168 samples of carbonaceous seriticitic phyllite from gold mine in Minas Gerais State, Brazil. Although gold is mainly associated with pyrite and arsenopyrite, there is a strong correlation between a higher proportion of gold associated with arsenopyrite with high exposure of accessible gold in this mineral.

Table 1 – Products and analysis.

Products	Analysis
Bulk sample 0.50–0.020 mm	XRF, S, As, Au Mineralogical analysis by XRD
Slimes −0.020 mm	Au, As and S
Sink (d > 3.3; 0.50 + 0.020 mm)	S, As, Au Mineralogical analysis and gold associations by SEM-IA
Flotation (P80: 107 µm)	As, Au – Gold Recovery
Cyanidation of flotation concentrate	

2. Materials and methods

2.1. Materials

The study was carried out in 168 samples from a gold mine in Minas Gerais State, Brazil. Each sample contained approximately 5 kg and was composed from a selected 1-m range of drill cores, respecting the limits of the range of the mineralized body.

The deposit is hosted in carbonaceous seriticitic phyllite with intercalation of phyllosilicate essentially composed by chlorite and millimeter of quartzite lenses. Sulphide in general are represented by pyrite, arsenopyrite and sparse occurrences of pyrrhotite, sphalerite, chalcopyrite and galena.

2.2. Methods

The detailed applied mineralogical studies of 168 samples comprised the comminution by roll crusher under 0.50 mm, which was the top size defined by initial textural analysis, homogenization and sampling of representative aliquots in a rotary divider for:

a) Sampling of head sample (<0.50 mm) for obtaining a representative aliquot;

Table 2 – Summary of chemical assays for fraction 0.50–0.020 mm (168 ore samples).

	SiO_2%	Al_2O_3%	Fe_2O_3%	Na_2O%	K_2O %	CaO %	MgO%	TiO_2%	LOI%
Mean	61.1	15.7	7.32	0.56	5.27	0.46	1.07	0.81	5.06
Median	60.4	15.6	7.60	0.53	5.28	0.47	1.12	0.82	5.28
Stdev	4.77	2.79	1.31	0.25	0.74	0.26	0.16	0.12	0.84
max	75.5	22.4	20.8	1.22	7.79	1.56	1.55	1.11	10.4
min	52.9	6.95	2.24	0.14	2.63	0.01	0.56	0.39	2.11

Stdev: standard deviation; max: maximum, min: minimum.

Table 3 – Summary of the chemical assays of sample (fraction 0.5 + 0.020 mm) and slimes (fraction −0.020 mm) 168 ore samples).

	Content			Distribution (%)			
	S %	As (ppm)	Au (g/t)	% weight	S	As	Au
Fraction 0.50 + 0.020 mm							
Mean	1.93	3467.0	0.880	69.9	86.9	80.4	93.4
Median	1.84	2122.0	0.516	71.7	88.2	86.8	95.2
Stdev	0.733	2865.8	1.42	8.99	5.78	19.5	5.45
max	5.04	3004.3	12.45	83.6	98.5	97.1	99.7
min	0.021	229.00	0.040	30.9	53.6	0.005	66.2
Fraction −0.020 mm							
Mean	0.77	1516	0.143	30.1	13.1	19.6	6.63
Median	0.62	704	0.100	28.3	11.8	13.1	4.80
Stdev	0.45	2472	0.174	8.99	5.73	19.5	5.43
max	2.42	16,207	1.49	69.1	46.4	97.1	33.8
min	0.01	0.08	0.001	16.3	1.46	0.005	0.267

Stdev: standard deviation; max: maximum, min: minimum.

b) Screening at 0.020 mm to remove the slimes;
c) Mineral separation by heavy liquid (specific gravity; SG = 3.30 g/cm^3) of the fraction 0.50 + 0.020 mm aiming to concentrate gold grains in sink product and increase statistical robustness of gold bearing minerals association [19]. The floated product was not subjected to the SEM-IA analysis due to the low concentration or absence of gold.

The attained products and analyses obtained were presented below (Table 1), in which 168 ore samples were considered for characterization and 34 selected samples for flotation and cyanidation from different point of the mine.

Chemical analysis was carried out by standardless XRF in fused beads (multielementar analysis – Panalytical Axios Advanced equipment), dosage of Au content by fire assay, As by ICP-OES and S by the pyrolysis method in an induction furnace with determination by infrared cell.

Mineralogical analysis for minerals identification was performed by XRD using the powder method with Cu kα radiation (D8 Endeavor diffractometer, from Bruker AXS). Quantitative mineralogy was assessed at 0.50–0.020 mm in polished sections by SEM-IA using the MLA/FEI software coupled to a FEI Quanta 600 FEG scanning electron microscope. The determination of the mineralogical composition, form of occurrence and associations of sulfides were done in extended BSE liberation analysis (XBSE).

Forms of occurrence and association of gold was carried out on sink products of heavy liquid separation in polished

Table 4 – Summary of the chemical assays of float and sink products (fraction 0.50 + 0.020 mm; 168 ore samples).

	Content			Distribution (%)			
	S %	As (ppm)	Au (g/t)	% weight	S	As	Au
Fraction 0.50 + 0.020 mm – Float at 3.3 g/cm^3							
Mean	0.113	335.5	0.177	88.8	8.70	15.1	18.9
Median	0.087	138.5	0.130	88.8	5.51	7.41	14.5
Stdev	0.090	705.3	0.168	5.75	7.63	18.2	15.4
max	0.513	6678.1	1.16	97.1	33.3	99.8	88.9
min	0.003	1.01	0.007	53.9	0.295	0.034	0.472
Fraction 0.50 + 0.020 mm – Sink at 3.3 g/cm^3							
Mean	16.61	25674.2	12.1	11.1	91.4	84.9	81.6
Median	16.89	14436.6	6.33	11.6	94.5	92.6	85.9
Stdev	8.42	34189.3	29.6	5.75	7.63	18.1	15.5
max	35.55	178845.5	333.6	46.1	100.0	99.9	100.0
min	0.079	217.2	0.107	2.97	66.6	0.105	11.0

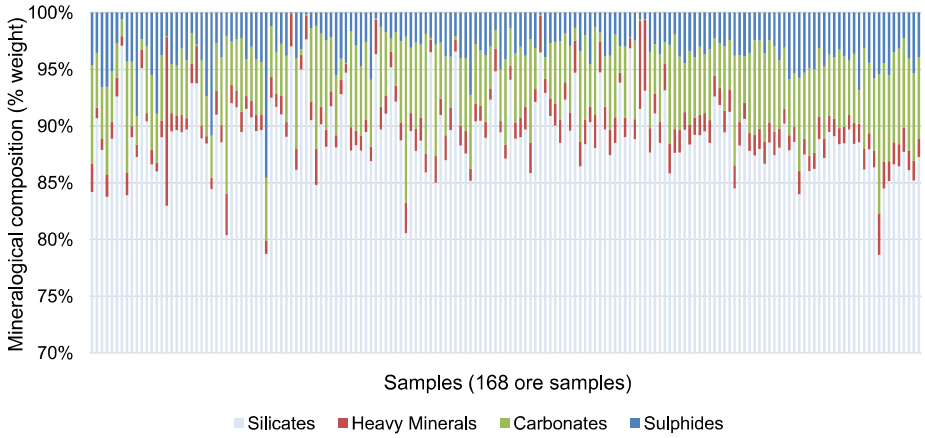

Silicates: Quartz, mica, albite and chlorite; Heavy Minerals: Ilmenite, goethite and rutile; Carbonates: siderite and anquerita; Sulphides: pyrite, pyrrhotite, arsenopyrite, chalcopyrite, sphalerite and galena.

Fig. 3 – Mineralogical composition of the samples by SEM-IA – 168 samples (fraction 0.50 + 0.020 mm, sink product).

sections using the MLA software coupled to a FEI Quanta 600 FEG scanning electron microscope, using sparse phase liberation (SPL) analysis. The automated search of the gold grains in polished sections of 30 mm in diameter relative to the heavy product with an analysis time of approximately 2.5 h section under the conditions of 300X. A specific database for the present study, containing data on specific weight, chemical composition and EDS spectrum, was created for all minerals present (mineral reference). In total, 551 polished sections were analyzed.

Laboratory flotation tests were conducted in parallel on selected 34 samples in a Denver laboratory flotation test machine model D12, with a nominal 3-L cell. In the rougher bulk sulphide stage, the pulp with 35% solids by weight, and pH 4.0 was conditioned in the impeller speed set at 1500 rpm for 9 min. P_{80} of 107 μm is the current grinding condition at the company. The reagents used in the tests were: PAX (Potassium Amyl Xanthate, dosage 15 μl), classic collector commonly used in sulphide flotation and AP 404, mixture of dithiophosphate and sodium mercaptobenzothiazole (dosage 12.8 μl) and Dowfroth 250 (DF 250, dosage 7.65 μl), polypropylene glycol type frother. In order to determine the gold recovery by direct cyanidation, the concentrate from flotation testwork was cyanided. The leaching parameters were: pre-conditioning of 1 h; dissolution period of 24 h; carbon addition of 10 g/L; cyanide addition of 3.5 kg/t; and variation of CaO addition to keep pH at 11.

3. Results and discussion

3.1. *Chemical composition and mineralogy*

The summary of the chemical composition of 168 ore samples are presented in Table 2, considering XRF for major elements.

The chemical composition reveals a highlight for high composition of SiO_2, varying from 52.9 to 75.5% (mean of 61.1%) and Al_2O_3 ranging from 6.95 to 22.4% (mean of 15.7%). These samples are composed exclusively of phyllites, which is consistent with the chemical composition presented in the summary table. Loss on ignition (LOI) results indicate the content of carbonates represented here by siderite and ankerite, which are predominant in the samples.

The fire assay for Au, pyrolysis for S and ICP-OES for As results and their distributions are showing in Table 3 for fraction 0.5 + 0.020 mm and −0.020 mm.

Table 5 – Summary of the mineralogical composition for 168 ore samples (fraction 0.5 + 0.020 mm, sink product).

	Silicates (%)				Heavy Minerals (%)			Carbonates (%)		Main sulphide (%)			
	qtz	mic	clt	alb	ilm	gth	rut	sid	anq	py	prt	aspy	gal
Mean	44.8	36.7	2.41	5.21	1.06	0.63	0.15	4.75	0.86	1.59	0.37	0.76	0.08
Median	42.6	37.7	1.54	4.16	1.05	0.41	0.14	4.62	0.88	1.51	0.21	0.40	0.01
Stdev	9.18	6.26	2.61	2.98	0.37	1.18	0.07	2.66	0.66	0.83	0.45	1.20	0.16
max	78.3	49.9	14.2	13.8	2.27	13.3	0.44	14.6	3.05	3.56	2.37	10.1	1.11
min	28.6	16.5	0.08	0.96	0.27	0.03	0.04	0.01	0.01	0.01	0.01	0.01	0.01

Stdev: standard deviation; max: maximum, min: minimum; qtz: quartz, mic: mica, clt: chlorite, alb: albite; ilm: Ilmenite, rut: rutile and gth: goethite; sid: siderite anq: anquerita; py: pyrite, prt: pyrrhotite, aspy: arsenopyrite, gal: galena.

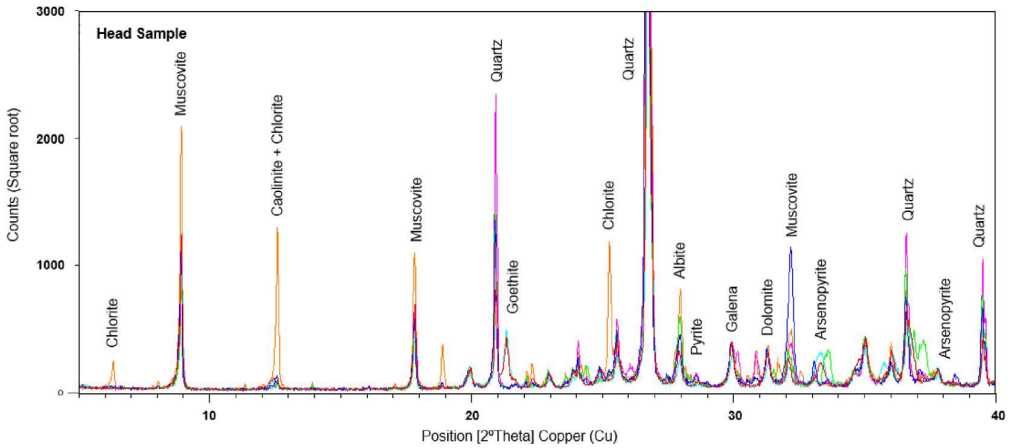

Annex 1 – Major mineral composition of the sample determined by XRD (Bulk Sample).

The sulfur content of the samples indicating high variability (0.02–5.04%) in the fraction 0.50 + 0.020 mm. On the fraction −0.020 mm, the sulfur ranges from 2.42 to 0.01%. Low sulfur grades indicate samples without or low gold probability. High mean on gold content occurs nugget effect in 5 samples (gold grade 12.45; 9.65; 6.27; 4.88 and 4.71 g/t), which displaced the averages to 0.880 g/t. The arsenic content of the samples was high (fraction 0.50–0.020 mm; maximum: 3004.3 ppm; minimum: 229.0 ppm), therefore arsenopyrite was expected to be present in major amounts. About 70% of the mass distribution is above 0.020 mm where 87% of S, 80.4% of As and almost all of gold (93.4%) are distributed. These results indicate that there is a very low distribution of gold in the finest fractions of the samples.

The float product represents on average 88% of the total mass of the sample and corresponds to 18.9% of the gold distribution in the sample. This product is mainly composed of silicates and carbonates. The distribution of arsenic and sulfur is also low (15.1 and 8.7%, respectively) possibly corresponding to some trailing sulfide mineral or in a finer granulometry.

Regarding the objective of concentrating gold for SEM-IA characterization, heavy liquid separation proved to be efficient for the considered ore, since there was a clear enrichment of Au, As and S at sink product compared to the initial fraction. The sink product of the 0.50 + 0.020 mm fraction is a concentrate with a high gold content (12.1 ppm) that corresponds to about 82% of the gold in the sample. The high concentration resulting from the separation of heavy liquid shows that the gold is mostly associated with sulfide or free mineral. Table 4 presents the results for the products float and sink resulting from the heavy liquid tests as well as their grades and distributions.

X-ray diffraction and SEM-IA mineralogy analysis were performed to obtain the detailed quantitative mineralogical composition of each sample. The mineralogical compositions determined by SEM-IA for the fraction 0.50–0.020 mm show the considerable presence of quartz, mica and albite, which together represent, on average, 85% of the total sample composition (Fig. 3 and Table 5). Sulfide minerals such as sphalerite and chalcopyrite were not represented in the table due to erratic occurrence.

Minor proportions of the following minerals were also detected: heavy minerals (goethite + ilmenite + rutile) (2%), chlorite (clinochlorine; 2.41%), arsenopyrite (0.76%), pyrite (1.59%), galena (0.08%) and pyrrhotite (0.37%), and very rarely

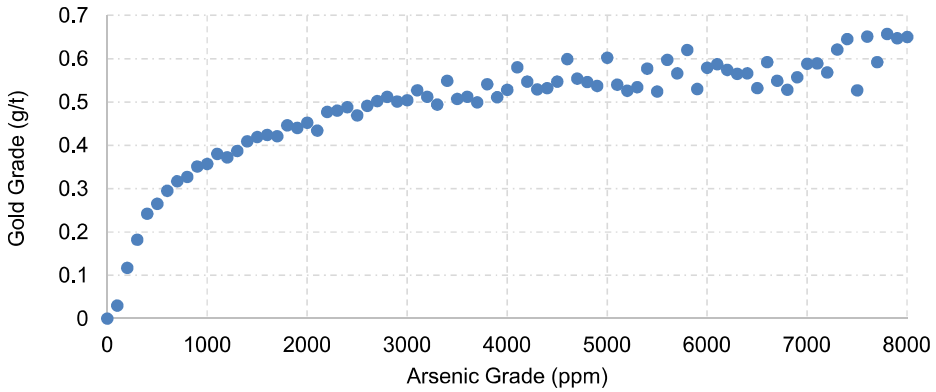

Fig. 4 – Relationship between arsenic and gold contents

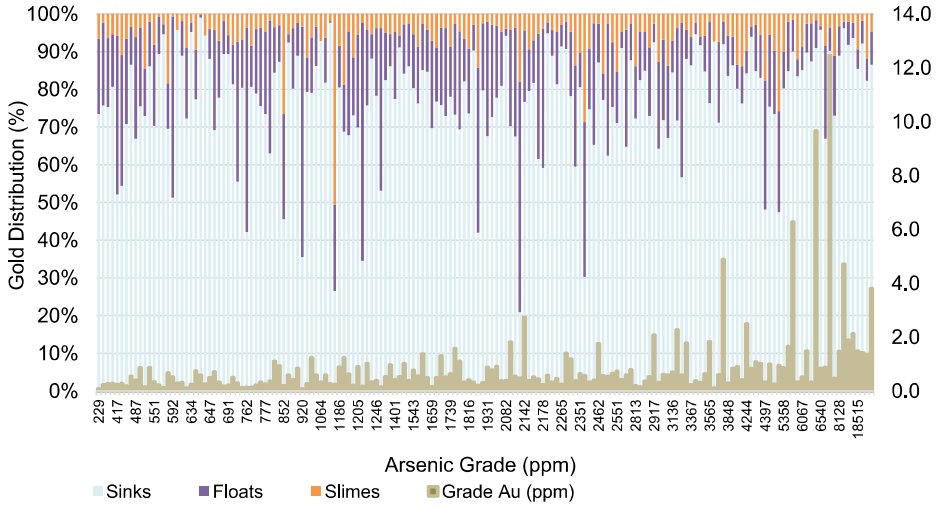

Fig. 5 – Gold distribution and grade on slime (−0.020 mm), float and sink products (0.50 + 0.020 mm; 168 samples)

chalcopyrite and sphalerite. Two varieties of carbonates, ankerite and siderite (5.61%; total), occurred in the samples in varying proportions.

The X-ray diffraction carried out in bulk sample supported the mineralogy assessed by the SEM-IA. The study area is formed exclusively by phyllites that vary in different proportions of the sulfide contents, which would explain the variation in the mineralogy in the diffractograms mainly in smaller minerals. The Annex 1 represents the overlap of eight representatives' samples at different positions in the mine.

3.2. *Relationship between arsenic and gold content*

Considering that arsenic grade is the key factor for the delimitation of mineralized areas and the relationships and distinctions between the types of ores for mining purposes, in this study we considered five classes of arsenic content (<1000; 1000–2000; 2000–3000; 3000–4000 and >4000 ppm). Arsenic (assessed by ICP–OES) and gold contents (in the range of 0–0.7 g/t of Au analyzed by fire assay) were considered.

The comparative data provide a relationship between gold and arsenic contents. A dispersed tendency of gold distribution is observed at higher levels of arsenic. This behavior can be interpreted as the effect of clusters, agglomerations or coarse-grained granules associated with arsenopyrite, according to the similar behavior shown in Fig. 4.

3.3. *Mineral separation and grain size distribution*

The proportion of gold in the products, obtained in the mineral's separation, can be a major factor in the metallurgical performance of gold ore. The results of heavy liquid separation

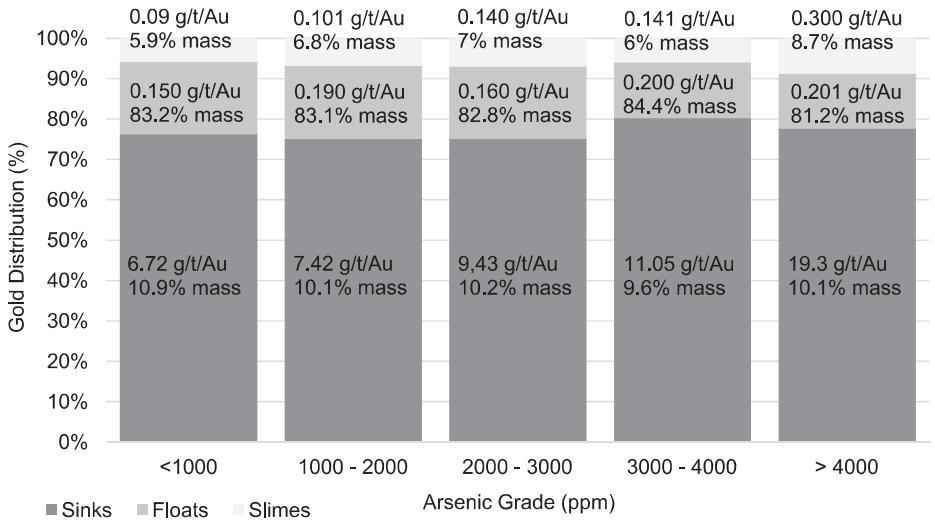

Fig. 6 – Gold grade and distribution on sink, float and slime products (0.50–0.020 mm; 168 samples).

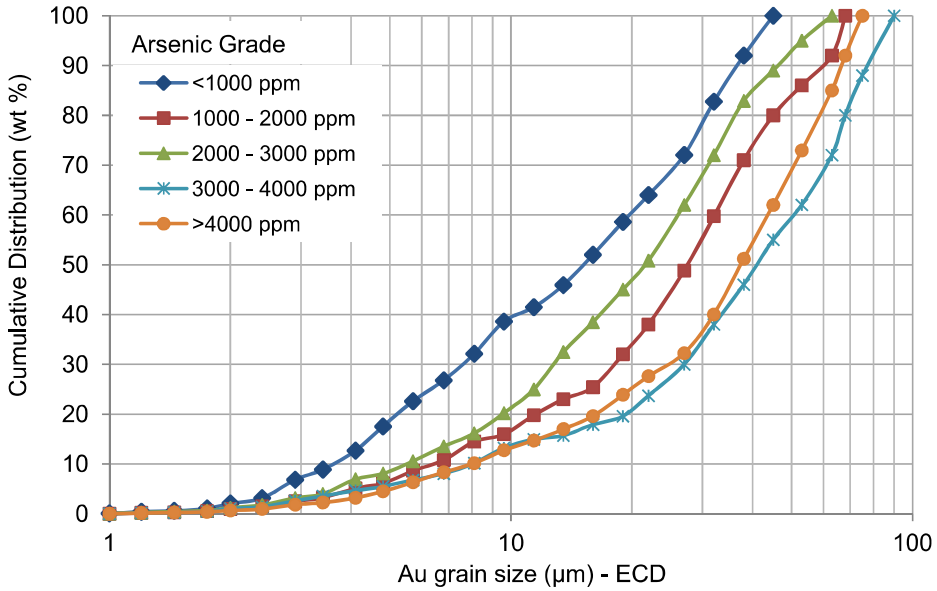

Fig. 7 – Gold grain size distribution (fraction 0.50 + 0.020 mm)

give an indication of the amenability of the to the gravity recovery. Gold reporting to the floats products is usually fine-grained associated with light gangue, such as quartz, mica and chlorite or still in carbonates.

Fig. 5 shows the distribution of gold in the slime (−0.020 mm), float and sink products (0.5 + 0.020 mm) as well as the gold grade in the 168 samples. Significant gold content corresponds to the sink product and sulphide ores where gold grains are concentrated. In some samples, the gold distribution is significant at float product possibly associated with silicates. It is also possible to notice the increasing of the gold content in the direction of high arsenic as well as the decrease in the distribution of gold in the float product. Slimes keep me the distribution of gold in all samples.

For better visualization and as a preponderant factor in the delimitation of the mineralized areas, Fig. 6 shows the distribution of gold in the slime, float and sink products grouped according to the arsenic content, characteristic of the deposit studied. The gold grade and distribution on sink and float products, as well as slimes grouped by arsenic grades.

Despite the fact that the gold distribution on the sink product presents little variation (from about ~76–~80%) with no clear tendency regarding the arsenic content, there is a notable increase in gold grades from 6.7 ppm in the As-group below 1000 ppm to 19.3 g/t of gold in the As-group >4000 ppm.

The float product corresponds to an 81.2–84.4% mass and approximately 20% of the gold distribution. The gold content increases along with the arsenic content from 0.150 to 0.201 ppm. The slime product corresponds to below 10% in the distribution of gold with a significant content in class >4000 ppm of arsenic.

The cumulative size distributions of gold grains by SEM-IA are displayed in Fig. 7. Considering the total sample (0.50–0.020 mm), the average gold grain diameter decreases along with the As content, being 17 μm for an arsenic grade <1000 ppm, 20–30 μm for an arsenic class between 1000 and 3000 ppm and 40 μm for an arsenic grade >3000 ppm. The size distribution may be quite heterogeneous not only in terms of gold distribution but also in terms of grain size and mineral associations. Coarse gold is indicated by high assay variability, high recovery by heavy liquid separation and gravity and a large portion of the gold grains >25 μm of ECD (equivalent circular diameter).

In total, 911.520 particles from 551 polished sections were identified by SEM-IA. Among them, 1.357 were gold bearing particles and 1.914 grains of gold. For the arsenic level >3000 ppm, the particles with gold increased due to the direct relationship with gold content. These results are shown in Table 6.

Table 6 – Total particles analyzed.

Arsenic Grade (ppm)	Gold Grade (ppm)	Total particles (TP)	Gold-bearing particles (GP)	Gold grains	GP/TP (%)
0–1000	0.492	204.751	686	1.099	0.33
1000–2000	0.613	206.846	1000	1.636	0.48
2000–3000	0.703	178.768	831	1.513	0.47
3000–4000	0.754	119.502	464	730	0.39
>4000	1.325	201.653	719	1.160	0.36

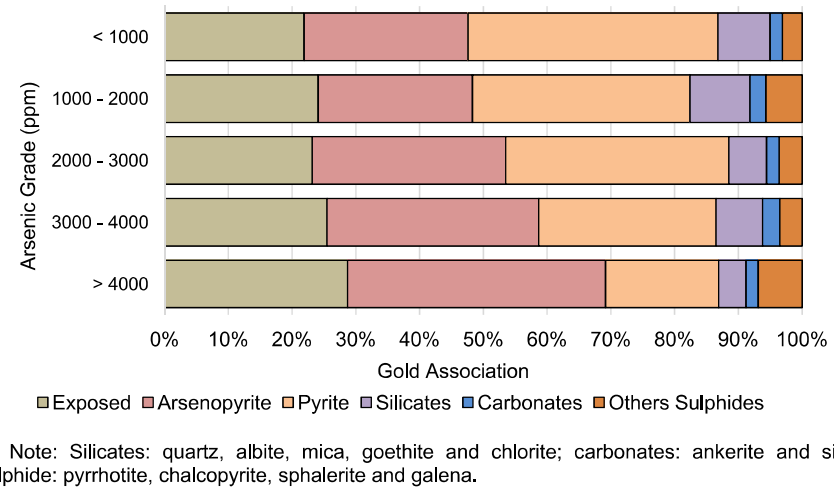

Note: Silicates: quartz, albite, mica, goethite and chlorite; carbonates: ankerite and siderite; Sulphide: pyrrhotite, chalcopyrite, sphalerite and galena.

Fig. 8 – Gold association from fraction 0.50 + 0.020 mm on the sink product. Note: Silicates: quartz, albite, mica, goethite and chlorite; carbonates: ankerite and siderite; Sulphide: pyrrhotite, chalcopyrite, sphalerite and galena.

3.4. *Mineral associations*

From a geometallurgical perspective, pyrite, arsenopyrite and pyrrhotite are the most important gold associations, with a small contribution in silicates (quartz, chlorite and mica), carbonates (anquerita) and other sulphide (chalcopyrite, sphalerite and galena). With the progressive increase of the arsenic content, an increment of gold associated with arsenopyrite occurs. The main aim of a gold association characterization is to describe and locate gold-bearing particles in order to determine the gold speciation. It should be emphasized that our mode of occurrence refers to mineral associations or gold accessibility.

The main gold associations, assessed by SEM-IA on the sink product (d > 3.30 g/cm^3), are shown in Fig. 8 and expressed in terms of perimeter of contact with other minerals. The gold with exposed perimeter on bearing particles accounts for 21.9% of the total gold perimeters for As-class <1000 ppm and increases to 29% for As-class >4000 ppm.

For classes with higher arsenic content, the occurrence of gold is mainly associated with arsenopyrite and pyrite, followed by carbonates and silicates, as well as a remarkable decrease of chlorite content.

3.5. *Accessibility and flotation tests*

In geometallurgical programs, the number of samples to be analyzed in the daily routine is high. The conditions for sample preparation and the time of analysis do not exclude the use of automated mineralogy to provide information in order to determine causes of different responses of minerals to various metallurgical processes. The information generated

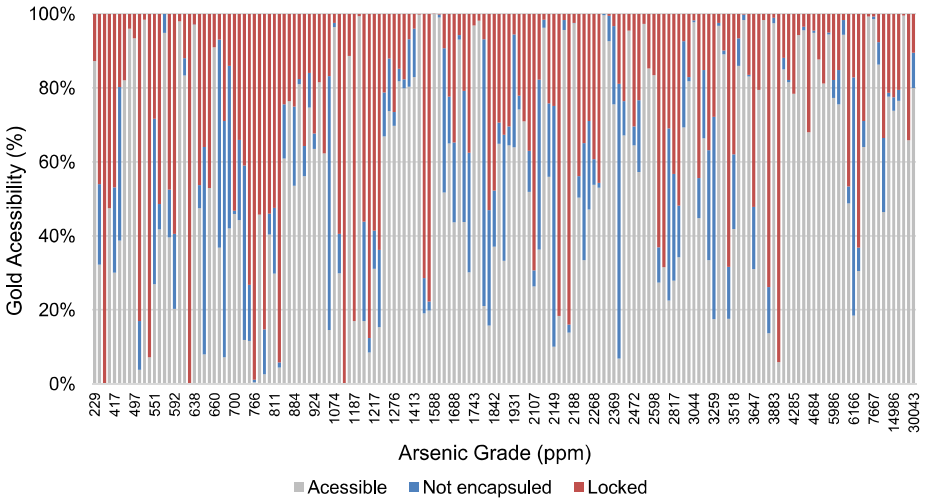

Fig. 9 – Accessible, non-encapsulated and locked gold from the contact perimeter of gold grains (sink product, fraction 0.50 + 0.020 mm) for 168 samples.

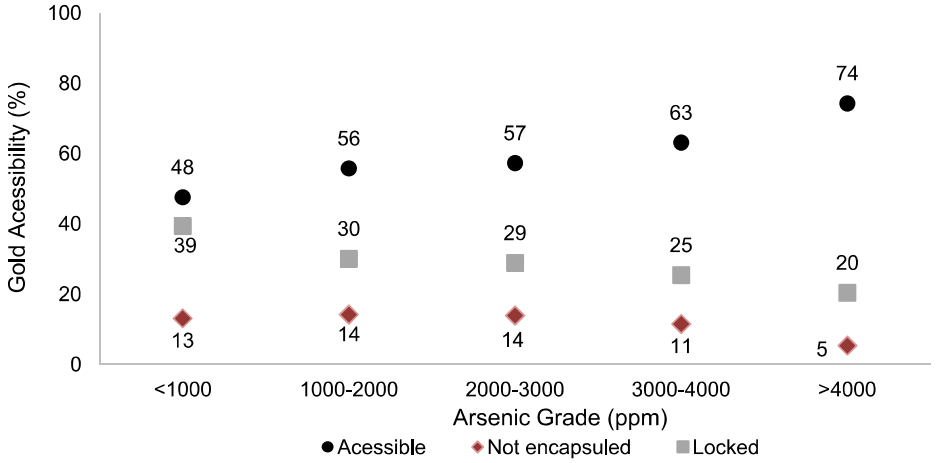

Fig. 10 – Accessible, non-encapsulated and locked gold from the contact perimeter of As-group (average; sink product, fraction 0.50 + 0.020 mm)

by detailed mineralogical associations by SEM-IA may contribute to an increase of predictability for mineral processing and deposit modeling in geometallurgy.

Considering each sample, the proportion of accessible gold shows a wide variation along the progressive increase in arsenic content as represented in Fig. 9. The gold accessibility area estimates revealed that the increase in arsenic zones exposed gold areas and reduced encapsulated and locked gold. In mineralized zones below 1000 ppm of arsenic content, 48% of the gold was accessible and liable to be recovered by direct cyanidation, consequently increasing this value to 63% and 74% in the area above 3000 and 4000 ppm, respectively (Fig. 10).

A detailed gold deportment study can be considered to avoid a considerable amount of time that would have been wasted on a test work program to recover the "locked" gold such as flotation, ultra-fine grinding and even high-pressure leaching. Ultra-fine grinding is a physical method for the liberation of locked gold with high energy requirements.

The flotation tests were conducted to recover the sulphide and gold. Flotation mass recovery is summarized in Fig. 11. The results indicate that around 10–12% of the total sample is reported to flotation concentrate, which is enriched in sulfide + gold (possibly free). The flotation results approximate the test with heavy liquid separation where the product from the sink resembles the flotation concentrate in which it represented about 10% (Fig. 6) of the average mass in the samples. One factor that may explain this difference is the greater accuracy in the heavy liquid test, which would generate a slightly lower mass.

Although the direct cyanidation test can indicate the amenability of the ore to gold extraction by direct leaching with results compared to the gold grain exposure determined during SEM-IA analysis, the grain accessibility does not give a clear indication of the leachability of an ore at a specific condition (34 samples analyzed). Herein, the recovery of gold in the direct leaching varied between 41.65 and 95.65% with an

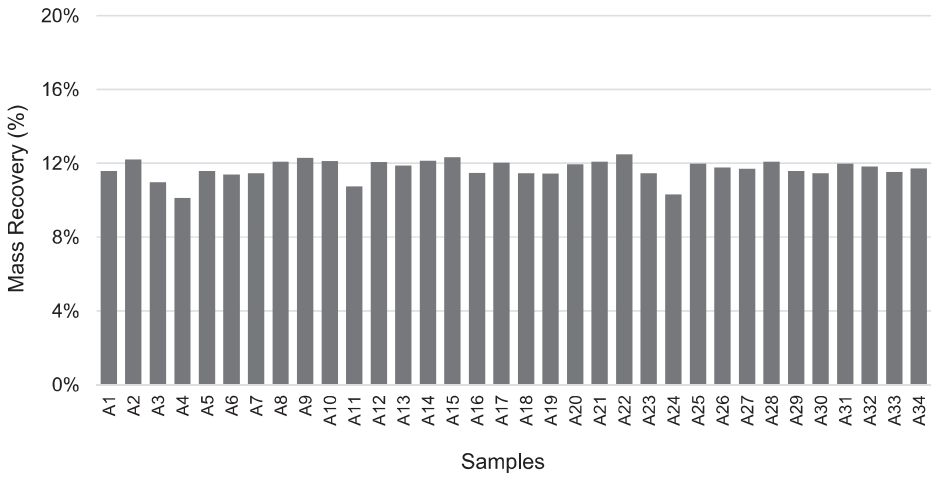

Fig. 11 – Mass recovery of flotation tests with 34 samples.

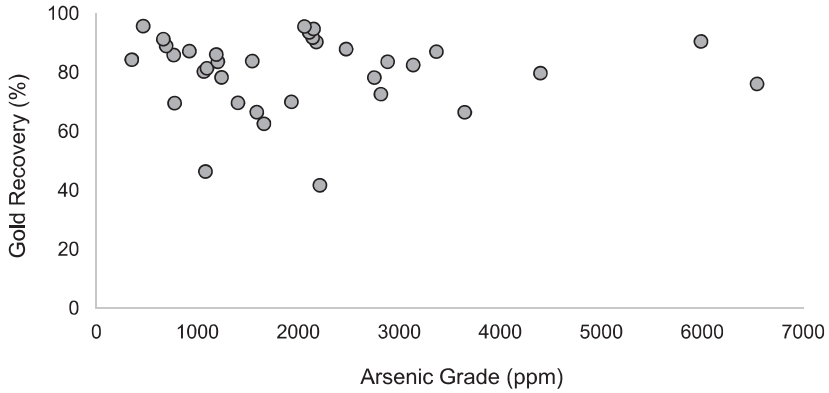

Fig. 12 – Gold recovery from cyanide leaching of flotation concentrate (34 samples, −0.50 mm).

average of 80% to 34 samples, as showed in Fig. 12. A possible cause of the low increase of gold recovery, below 80% is attributed to the use of cyanide addition control (3.5 kg/t). An intense cyanidation leaching is recommended in high grades and exposed gold grains. Furthermore, coarse gold found primarily at high arsenic levels, as shown in Fig. 7 could be a reason for poor gold recovery, as it requires longer retention times during cyanidation in order to achieve full dissolution or adequate leaching kinetics otherwise, partial dissolution of coarse gold leads to gold losses to the tailings. More intensive leach conditions such as longer retention times, more cyanide and higher dissolved oxygen may be required to improve gold recovery. Additionally, 34 from 168 samples were submitted to flotation and cyanidation tests.

4. Conclusion

The study regarding the identification of differences in the mineralogical composition of gold and especially the gold associations was conducted to assist the development or optimization of the process flowsheet. For this purpose, an automated image analysis by SEM was performed to enable this quantification with statistical robustness and in the shortest time possible.

The combination of pre-concentration stage and the use of an SEM-IA automated tool proved to be particularly efficient for the number of particles analyzed and the gold grade determination of the exposed perimeter, thus being suitable for geometallurgy for the analysis of mineral as a way to support the predictive geological block model and mineral processes by incorporating these aspects into industrial mineral operations. As described in the literature, the geometallurgy challenges related to the heterogeneity of the ore prompted systematic obtained data, endeavouring to improve mineral resource intelligence.

The results demonstrated that ore bodies with a high content of arsenic (4000 ppm) showed enhanced gold accessibility of approximately 26% when compared to grades below 1000 ppm, as well as a substantial increase in the average size of the gold grains, evidencing a potential increase in recovery due to the high exposure of gold in a cyanide solution.

Credit author statement

Fabrizzio R. Costa – methodology, investigation, writing – original draft, **Guilherme P. Nery** – methodology, validation, investigation, **Cleyton de Carvalho Carneiro** - writing - review & editing, visualization, **Henrique Kahn** – conceptualization, methodology, validation, writing - review & editing, **Carina Ulsen** - conceptualization, methodology, resources, writing - review & editing, project administration, funding, writing - review & editing.

Declaration of Competing Interest

The authors declare that they have no known competing financial interests or personal relationships that could have appeared to influence the work reported in this paper.

Acknowledgments

We would like to thank the technical team from the Technological Characterization Laboratory of the Polytechnic School at the University of São Paulo (USP) for their analytical support, and the scholarship offered by the Coordination for the Improvement of Higher Education Personnel (CAPES) to F.R. Costa and G. P. Nery. The authors would also like to thank the anonymous referee for reviewing the manuscript and providing valuable comments and suggestions.

REFERENCES

[1] Lane GR, Martin C, Pirard E. Techniques and applications for predictive metallurgy and ore characterization using optical image analysis. Miner Eng 2008;21:568–77. https://doi.org/10.1016/j.mineng.2007.11.009.

[2] Lamberg P. Particles – the bridge between geology and metallurgy: conference in mineral engineering, Luleå, Sweden, 8-9 February. Proceedings 2011:1–16.

[3] Suther SP, Pownceby MI, Manuel J, Ware N, Donskoi E, Poliakov A. Geometallurgical characterization of Australian

iron ores - from ore to processed product. 6-7 September. In: Metallurgical plant design and operating strategie (MetPlant); 2004. p. 351–60. Perth, WA, Australia.
[4] Lishchuk V, Koch PH, Ghornabi Y, Butcher AR. Towards integrated geometallurgical approach: critical review of current practice and future trends. Miner Eng 2020;145:1–16. https://doi.org/10.1016/j.mineng.2019.106072.
[5] Lotter NO. Modern process mineralogy: an integrated multi-disciplined approach to flowsheeting. Miner Eng 2011;24:1229–37. https://doi.org/10.1016/j.mineng.2011.03.004.
[6] Evans CL, Wightman EM, Manlapig EV, Coulter BL. Application of process mineralogy as a tool in sustainable processing. Miner Eng 2011;24:1242–8. https://doi.org/10.1016/j.mineng.2011.03.017.
[7] Lang AM, Aasly K, Ellefmo SL. Mineral characterization as a tool in the implementation of geometallurgy into industrial mineral mining. Miner Eng 2018;116:114–22. https://doi.org/10.1016/j.mineng.2017.10.021.
[8] Lamberg P, Lund C. Taking liberation information into a geometallurgical model-case study, Malmberget, Northern Sweden. 7-9 November; Cape Town, South Africa. In: Process Mineralogy' 12; 2012. p. 1–13. Proceedings.
[9] Lund C, Lamberg P. Geometallurgy – a tool for better resource efficiency. Topic – metallic Minerals. Eur Geol 2014;37:39–43.
[10] Koch PK, Rosenkranz J. Sequential decision-making in mining and processing based on geometallurgical inputs. Miner Eng 2020;149:1–10. https://doi.org/10.1016/j.mineng.2020.106262.
[11] Henley KJ. Ore-Dressing Mineralogy - a review of techniques, applications and recent developments. Geol Soc South Africa 1983;7(7):175–200.
[12] Barbery G. Mineral liberation, measurement, simulation, and practical, use in mineral processing. 1991. p. 351. Les Editions GB, C.P. 38025, Quebec, Canada.
[13] Jones MP, Shaw JL. Automatic measurement and stereological assessment of mineral data for use in mineral technology. In: Jones MP, editor. Proceedings of the tenth international mineral processing congress. London: Institution of Mining and Metallurgy; 1974. p. 737–56.
[14] Gaudin AM. Principles of mineral dressing. New Delhi: Tata McGraw Hill; 1939. p. 554.
[15] Petruk W. Applied mineralogy in the mining industry. Amsterdam; New York: Elsevier Science BV; 2000.
[16] Coetzee LL, Theron SJ, Martin GJ, Merwe JDV, Stanek TA. Modern gold deportments and its application to industry. Miner Eng 2011;24:565–75. https://doi.org/10.1016/j.mineng.2010.09.001.
[17] Cook NJ, Chryssoulis SL. Concentrations of "invisible" gold in common sulfides. Can Mineral 1990;28(1):1–16.
[18] Goodal WR, Scales PJ. An overview of the advantages and disadvantages of the determination of gold mineralogy by automated mineralogy. Miner Eng 2007;20:506–17. https://doi.org/10.1016/j.mineng.2007.01.010.
[19] Costa FR, Nery GP, Antoniassi JL, Ulsen C. Effective density concentration in refractory gold ore for characterization purposes. REM Int. Eng. J. 2020;73(4). https://doi.org/10.1590/0370-44672020730031.

Fabrizzio R Costa is a PhD candidate in the Mining and Petroleum Engineering Department at Sao Paulo University. His research interests focus on minerals processing, development and implementation of quantitative analytical methods to characterize the mineralogy and texture of ores with the production of several articles on the subject.

In addition, he has experience in gold and bauxite mining operations with a focus on short-term mining development and mine planning.